JACS
JOURNAL OF THE AMERICAN CHEMICAL SOCIETY

ARTICLE

pubs.acs.org/JACS

Effect of Substrate Inhibition and Cooperativity on the Electrochemical Responses of Glucose Dehydrogenase. Kinetic Characterization of Wild and Mutant Types

Fabien Durand,[‡] Benoît Limoges,[*,†] Nicolas Mano,[‡] François Mavré,[†] Rebeca Miranda-Castro,[†] and Jean-Michel Savéant[*,†]

[†]Laboratoire d'Electrochimie Moléculaire, UMR 7591 CNRS, Université Paris Diderot, Sorbonne Paris Cité, 15 rue Jean-Antoine de Baïf, F-75205 Paris Cedex 13, France

[‡]Centre de Recherche Paul Pascal, Université de Bordeaux, UPR 8641, Avenue Albert Schweitzer, 33600 Pessac, France

Supporting Information

ABSTRACT: Thanks to its insensitivity to dioxygen and to its good catalytic reactivity, and in spite of its poor substrate selectivity, quinoprotein glucose dehydrogenase (PQQ-GDH) plays a prominent role among the redox enzymes that can be used for analytical purposes, such as glucose detection, enzyme-based bioaffinity assays, and the design of biofuel cells. A detailed kinetic analysis of the electrochemical catalytic responses, leading to an unambiguous characterization of each individual steps, seems a priori intractable in view of the interference, on top of the usual ping−pong mechanism, of substrate inhibition and of cooperativity effects between the two identical subunits of the enzyme. Based on simplifications suggested by extended knowledge previously acquired by standard homogeneous kinetics, it is shown that analysis of the catalytic responses obtained by means of electrochemical nondestructive techniques, such as cyclic voltammetry, with ferrocene methanol as a mediator, does allow a full characterization of all individual steps of the catalytic reaction, including substrate inhibition and cooperativity and, thus, allows to decipher the reason that makes the enzyme more efficient when the neighboring subunit is filled with a glucose molecule. As a first practical illustration of this electrochemical approach, comparison of the native enzyme responses with those of a mutant (in which the asparagine amino acid in position 428 has been replaced by a cysteine residue) allowed identification of the elementary steps that makes the mutant type more efficient than the wild type when cooperativity between the two subunits takes place, which is observed at large mediator and substrate concentrations. A route is thus opened to structure−reactivity relationships and therefore to mutagenesis strategies aiming at better performances in terms of catalytic responses and/or substrate selectivity.

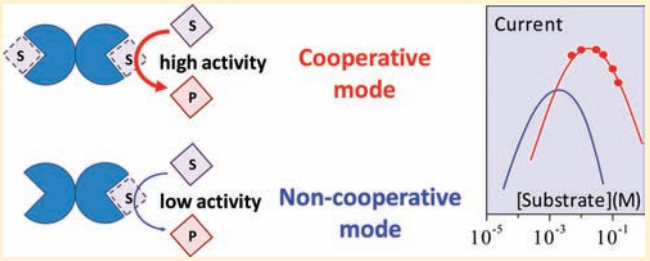

INTRODUCTION

Applications of electrochemical enzymatic catalysis by redox enzymes immobilized on the electrode surface or dispersed in solution are of two main types. The first of these encompasses two domains: One involves sensing the enzyme substrate by means of the catalytic current, electron transfer between the electrode and the enzyme being either direct or through a mediator that functions as cosubstrate to the enzyme.[1] A second domain relates to affinity biosensing (as, for example, in electrochemical immuno-, DNA-, and apta-sensors). One of the two complementary molecules is immobilized on the electrode surface, while the other member of the couple stands in the solution after being labeled by a redox active molecule.[2] In this framework, enzyme labeling is a powerful manner of amplifying the electrochemical response compared to simple redox labels.[3] Another type of application, which has attracted a lot of recent attention, concerns enzyme biofuel cells even though many problems still have to be solved as to real applications, performances, and durability.[4]

The rational design and testing of reproducible systems in these areas call for development and effective use of theoretical tools required for rigorously relating the electrochemical responses to the mechanism and the kinetic characteristics of the enzymatic reaction in the framework of a given electrochemical technique. These theoretical tools are available for ping−pong mechanisms in which the two half-reactions follow Michaelis−Menten kinetics,[5] and their application has been illustrated by several experimental examples.[5a,d,6] Addressing, from a theoretical standpoint, more complex reaction sequences particularly those involving substrate or product inhibition is scarce. The most notable exception to this state of affairs concerns substrate

Received: May 20, 2011
Published: July 25, 2011

inhibition occurring with horseradish peroxidase.[7] The effect of inhibition is important in sensor applications of this enzyme, since the calibration curves are strongly nonlinear, eventually exhibiting inverted concentration dependence. Inhibition is coupled with a slow regeneration step that makes the horseradish peroxidase mechanism appear as more of a case story than an illustrating example of a general theoretical issue. These are the reasons that we deemed important to examine the effect on electrochemical responses of more conventional substrate inhibition reactions, such as those that are encountered with quinoprotein glucose dehydrogenase (PQQ-GDH). Soluble PQQ-GDH from *Acinetobacter calcoaceticus* is a homodimeric enzyme constituted by two subunits of 50 kDa,[8] each containing one pyrroloquinoline quinone (PQQ) as a prosthetic group (Scheme 1).[9] Enzymatic reduction of PQQ involves the transfer of two electrons and two protons. The enzyme also contains six Ca^{2+} ions, four of them being involved in the dimerization of the subunits and the two others in the activation of the two PQQ molecules.[9,11] Soluble PQQ-GDH has been isolated from the bacterium *A. calcoaceticus* in the dimeric holoform[12] and in the dimeric apoform from an overproducing *Escherichia coli* recombinant strain.[13] Apo-GDH can be fully reconstituted in the dimeric holoform in the presence of PQQ and Ca^{2+}.[13] PQQ-GDH has a broad specificity toward the oxidation of aldose sugars (hexoses, pentoses, mono- and disaccharides) into the corresponding lactones and the reduction of artificial electron acceptors. It has a particularly high catalytic activity toward glucose, with a turnover number (k_{cat}) of 1550 s^{-1} and a catalytic efficiency k_{cat}/K_M, (K_M being the substrate Michaelis constant) of 2.1×10^6 M^{-1} s^{-1},[14] which are 2 and 200 times larger than in glucose oxidase (750 s^{-1} and 1.1×10^4 M^{-1} s^{-1}, respectively).[15] Because of this fast kinetics and also because of its insensitivity to dioxygen and broad acceptance of artificial electron acceptors, PQQ-GDH has been recommended as a substitute to glucose oxidase for improving the performances of amperometric glucose biosensors.[16] Various kinds of amperometric glucose biosensors with PQQ-GDH immobilized on an electrode surface have thus been developed, some of them employing diffusional redox mediator,[16,17] such as ferrocene derivatives,[16] and others using coimmobilized redox polymers,[18] such as osmium$^{III/II}$ poly(vinylpyridine) complexes.[18a,b] Several GDH-based glucose biosensors are currently commercialized for self-monitoring of blood glucose.[19] The PQQ-GDH has however the serious drawback to be less substrate-specific than glucose oxidase. In addition to glucose, it is able to catalyze the oxidation of several mono- and disaccharides, such as galactose, lactose, xylose, and maltose. This lack of specificity is a possible source of overestimating blood glucose levels. Improving substrate specificity of PQQ-GDH is therefore highly desirable for producing a more reliable self-monitoring PQQ-GDH-based blood glucose sensor. Enzyme engineering of PQQ-GDH by site-directed mutagenesis has thus been proposed as a viable strategy for improving the PQQ-GDH substrate specificity[20] and also its catalytic efficiency[21] and/or thermal stability.[22]

The high efficiency and oxygen insensitivity of PQQ-GDH can also be advantageously exploited in the development of dual-enzyme-based electrochemical biosensors.[23] For example, an improved adenosine-5′-triphosphate (ATP) microbiosensor based on co-immobilization of hexokinase and PQQ-GDH on an electrode surface was demonstrated, reaching submicromolar detection of ATP in biological fluids.[23b]

Scheme 1. Soluble PQQ-GDH from *Acinetobacter calcoaceticus*[a]

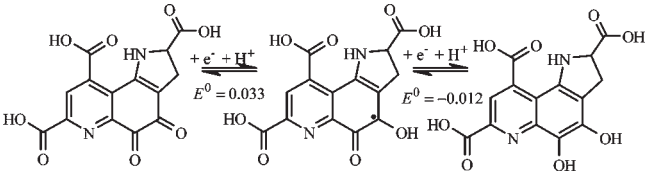

[a] Standard potentials in V vs SHE at pH of 7, in the same conditions as in the experiments reported here from ref 10.

Because of its high turnover number, PQQ-GDH has also been proposed as an enzyme label for the development of sensitive electrochemical enzyme-amplified bioaffinity assays. It has, for example, been applied to the amperometric detection of DNA hybrids[24] or sandwich DNA aptamers at the surface of a carbon electrode.[25] More recently, the possibility to efficiently and rapidly reconstitute the PQQ-GDH from the binding of the cofactor to the apo-glucose dehydrogenase form (apo-GDH) has been cleverly exploited as a simple and highly sensitive tracer system in a variety of bioaffinity binding assays.[26] When coupled to appropriate enzyme systems, PQQ-GDH can also be used as a very powerful reagent for amplifying the electrochemical response of biosensors by means of cosubstrate recycling.[27]

Thanks to its high turnover number, broad sugar reactivity, insensitivity to dioxygen, and fair stability, PQQ-GDH is also considered for the development of enzyme-based biofuel cells.[28] Genetic engineering of PQQ-GDH appears promising for improving the performances of this enzyme, in terms of stability[28b] and power density.

So far, GDH-based electrodes have been essentially developed empirically with no attempt to precisely establish the relationship linking the catalytic current to the glucose concentration. In this connection, establishing the mechanism and kinetic characteristics of the enzyme reaction and the role of the substrate and cosubstrate mass transport are important objectives. Equally important would be a systematic examination of the role that substrate inhibition, evidenced in previous spectrophotometric kinetic studies, may play in electrocatalytic responses.[12c,13,29] Steady-state and transient kinetic studies provided evidence for a ping−pong mechanism.[12b,c] Additional investigations with glucose as substrate and a *N*-methyl-phenazonium methyl sulfate/dichloroindophenol mix as cosubstrate revealed significant substrate inhibition and cooperativity between subunits at high sugar concentrations.[14,29] Although quite a number of PQQ-GDH-based amperometric glucose biosensors have been described, the effect of substrate inhibition and cooperativity on the current response and its consequence on the analytical performances (dynamic range, sensitivity, reliability, etc.) has only been occasionally evoked[27a] but never fully analyzed.

In illustrating the role of substrate inhibition by the example of PQQ-GDH, we examined the cyclic voltammetric responses obtained with the enzyme in solution and with a one-electron cosubstrate (ferrocene methanol, FcMeOH). The possibility that substrate inhibition could interfere at various points of the reaction scheme as well as the necessity to take cooperativity into account requires an analysis of somewhat complex catalysis kinetics in order to determine the numerous rate constants involved. The achievement of such a task in the illustrating case

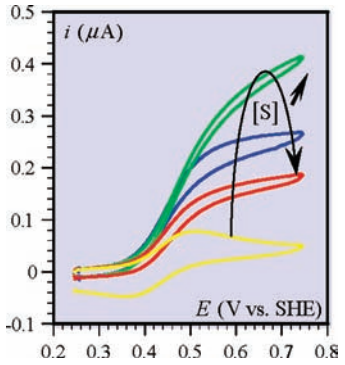

Figure 1. Catalysis of glucose oxidation by PQQ-GDH (wild type) with ferrocene methanol as mediator. Cyclic voltammetry at a screen-printed carbon electrode in 0.1 M of phosphate buffer (pH = 7) containing 1 g/L of BSA, 94 nM of PQQ-GDH, 3 μM of FcMeOH, and variable concentrations of D-glucose: 0 (yellow), 0.03 (blue), 1 (green), 100 (red) mM. Scan rate: 0.1 V/s. Temperature: 20 °C.

of PQQ-GDH provides guidelines for strategies applicable to other enzymes exhibiting substrate inhibition and/or cooperativity.

As far as PQQ-GDH is concerned, the kinetic analysis allows one to characterize and explain quantitatively how substrate inhibition induces nonmonotonic substrate calibration curves, an important issue in all analytical applications.

Another illustration of the usefulness of the kinetic analysis, we contrast the behavior of the wild type of PQQ-GDH with one of its mutants and show how dissecting the kinetics into the various individual rate constants allows one to identify precisely the reactions that underlie the overall kinetic difference between the two enzymes.

RESULTS

Scan rates and concentrations of mediator and substrate were selected so as to obtain plateau- rather than peak-shaped cyclic voltammetric responses, corresponding to situations where the overall enzymatic reaction is rate determining, being slower than the diffusive transports of the mediator and the substrate.[30] Typical cyclic voltammograms are shown in Figure 1. Bovine serum albumin (BSA) was added to the solution in order to minimize adsorption of the enzyme on the electrode surface. As a preliminary observation, Figure 1 shows a typical example of substrate inhibition; the catalytic current first increases with substrate concentration, then passes through a maximum before decreasing upon further increase of substrate concentration. More generally, the concentration of mediator and substrate was varied systematically within the intervals where plateau-shaped current−potential responses were obtained so as to provide the least cumbersome and the most accurate kinetic analysis leading to the key rate constants. The variations of the plateau current with mediator and substrate concentration thus obtained are gathered in Figure 2. Gathering this large amount of data was made possible because in these electrochemical experiments, the enzyme reaction is started only when the potential is applied and not just after mixing as in conventional homogeneous kinetic experiments. Another favorable factor is the sensitivity of the electrochemical technique, which allows working at low mediator (cosubstrate) concentrations, down to the submicromolar range.

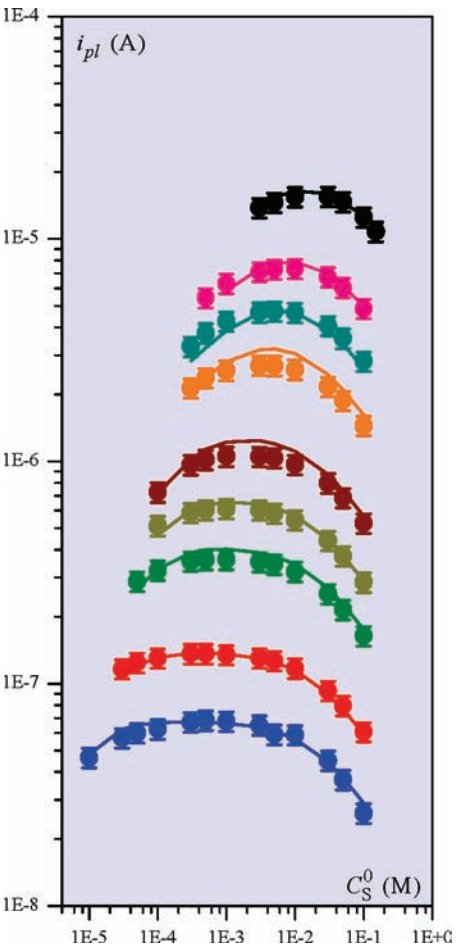

Figure 2. Catalytic plateau currents as a function of D-glucose concentration in the presence of 94 nM of PQQ-GDH (wild type) in 0.1 M of phosphate buffer (pH = 7) and various concentrations of FcMeOH (from bottom to top): 0.5, 1, 3, 5, 10, 30, 50, 100, and 300 μM, in the presence of 1 g/L of BSA. Temperature: 20 °C. Error bars: twice the average standard deviation (10%), corresponding to a 95% confidence interval based on 3 measurements. Full lines: theoretical curves (see text).

The same set of experiments was repeated with the mutant N428C of the enzyme obtained by introduction of a cysteine residue at position 428 instead of asparagine, albeit with a more restricted exploration of the effect of substrate and mediator. It is seen in Figure 3 that, at relatively high concentrations of mediator and substrate, catalysis by the mutant type may be more efficient than with the wild type.

Figure 4 compares the catalytic plateau current changes of the mutant- and wild- type enzymes with substrate concentration for two characteristic mediator concentrations. At high [FcMeOH], where cooperativity effects are expected (see below), the catalytic current is significantly higher with the mutant (right graph). On the contrary, at low mediator concentrations, the responses are practically the same.

DISCUSSION

Simplifying Assumptions and Operational Reaction Scheme. Based on previously gathered knowledge,[12b,31] several assumptions can be made that render tractable the full kinetic

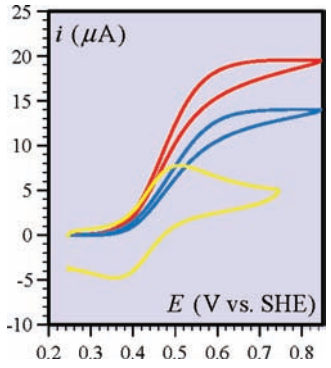

Figure 3. Comparison of catalysis of glucose oxidation by the N428C mutant (red) and the wild type (blue) of PQQ-GDH in the presence of ferrocene methanol as mediator. Cyclic voltammetry at a screen-printed carbon electrode in 0.1 M of phosphate buffer (pH = 7) containing 1 g/L of BSA, 94 nM of PQQ-GDH (wild and mutant types), 300 μM of FcMeOH, and 50 mM of D-glucose. Yellow: FcMeOH alone. Scan rate: 0.1 V/s. Temperature: 20 °C.

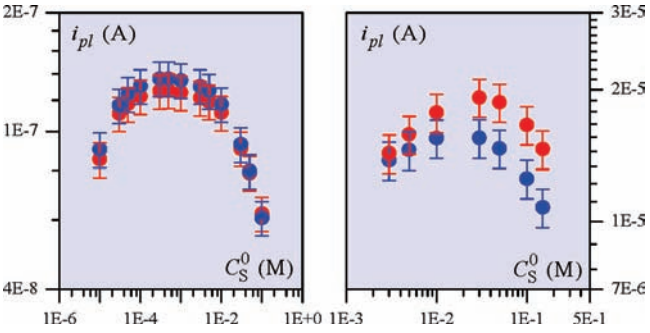

Figure 4. Catalytic plateau currents as a function of D-glucose concentration in the presence of 94 nM PQQ-GDH (blue: wild type; red: mutant N428C) in 0.1 M of phosphate buffer (pH = 7) and for two concentrations of FcMeOH (μM): 1 (left) and 300 (right). Error bars: twice the average standard deviation (10%), corresponding to a 95% confidence interval based on three measurements. Temperature: 20 °C.

analysis of the experimental data by means of a simplified operational reaction scheme (Scheme 2). The various simplifying assumptions are as follows: (i) In the oxidation half-reaction of PQQ-GDH by the oxidized form Q of ferrocene methanol (standard potential: 0.435 V vs SHE),[32] the semiquinone is oxidized somewhat less rapidly than the hydroquinone in view of the corresponding standard potentials of the two redox couples (Scheme 1). However, the large driving force of these reactions implies that they may be treated as simple bimolecular steps (close to diffusion control). Semiquinone intermediates may therefore be formally ignored in the kinetic analysis, leading thus to the redox processes represented in Scheme 2, which involves two-electron plus two-proton exchanges. (ii) Inhibition is assumed to affect only reduced forms of the enzyme, as pictured in Scheme 2. This assumption simply derives from the observation that when the substrate is associated with an oxidized form of any of the subunits, it undergoes oxidation, thus giving rise to a reduced form that may itself be associated with the substrate giving rise to inhibition. (iii): The rate constants in the reaction triangles 1 and 2 in Scheme 2 are regarded as being approximately the same, as a result of the likely assumption that the reactivity of each subunit is changed only

Scheme 2

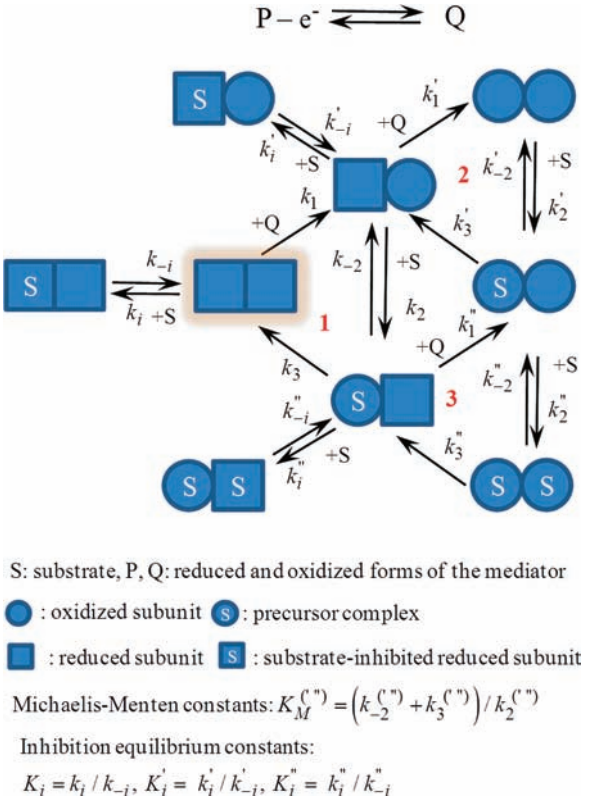

when the adjacent subunit is associated with the substrate under the form of a precursor complex.[31] For the same reason, the inhibition constants, $K_i = k_i/k_{-i}$ and $K_i' = k_i'/k_{-i}'$, are likely to be practically the same.

A general approach to the kinetic treatment of the catalytic reaction represented by Scheme 2 consists in applying the steady-state approximation to all enzyme forms, including inhibited forms. The applicability of the steady-state approximation to the inhibited forms of the enzyme results from the observation that the catalytic currents do not show any tendency to decrease within the time scale of the experiment. Under these conditions, the application of the steady-state approximation results in the contribution of inhibition reactions to the overall kinetics by their equilibrium constants rather than by their rate constants (see examples in the Supporting Information).

Closed-form expressions of the plateau currents, which would allow obtaining a reliably unique set of rate constant values, demonstrate a dissuasive complexity. Our strategy was therefore to define and treat limiting cases in which the general reaction scheme (Scheme 2) is reduced to one of the reaction triangles, the analysis of which will then also lead to a reliably unique set of rate constants. Note that the initial form of the enzyme in the presence of glucose is its doubly reduced form (shaded in orange) in equilibrium with its inhibited form.

Limiting cases: Determination of the Rate Constants. Two limiting situations are worth considering corresponding to small and large mediator concentrations, respectively.

Small Mediator Concentrations. If, by reference to Scheme 2, the mediator concentration, C_P^0, is small enough to fulfill the following conditions: $C_P^0 < k_3/k_1''$ and $k_2 C_S^0 / k_1'$, the global reaction scheme simplifies so as to be reduced to the reaction

Scheme 3

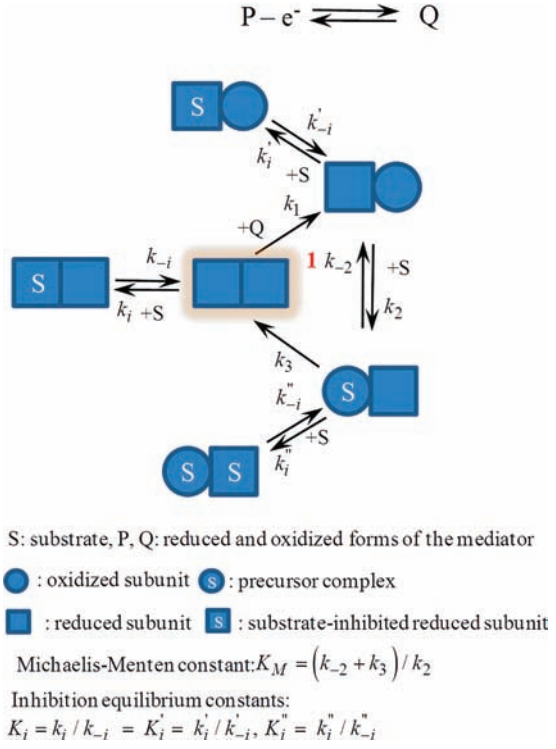

triangle 1, resulting in Scheme 3. It is worth noting that in this limiting case, cooperative effects are absent. The reaction scheme then simply corresponds to a standard ping−pong mechanism with substrate inhibition of all enzyme forms.

After application of the steady-state approximation to all enzyme forms, the plateau current, i_{pl}, is given by a closed-form expression (see Supporting Information):

$$\frac{i_{pl}}{FSC_P^0} = \sqrt{\frac{2k_1C_E^0D_P}{1 + K_iC_S^0}}\sqrt{\frac{2}{\sigma}\left[1 - \frac{\ln(1+\sigma)}{\sigma}\right]} \qquad (1)$$

with

$$\sigma = k_1C_P^0\left(\frac{1 + K_i''C_S^0}{k_3} + \frac{K_M(1 + K_iC_S^0)}{k_3C_S^0}\right)$$

where S (0.126 cm^2) is the electrode surface area, D_P, the mediator diffusion coefficient (6.7×10^{-6} cm^2s^{-1}), and C_P^0, C_S^0, C_E^0, the bulk concentrations of mediator, substrate, and enzyme, respectively. The rate and equilibrium constants are defined in Scheme 3.

The experimental data corresponding to these conditions are gathered in Figure 5. Do we have the necessary number of observables to determine unambiguously the constants involved in reaction triangle 1? To answer this question, we examine asymptotic situations obtained for extreme values of substrate concentration. Even though these asymptotes are not quite reached within the available range of substrate concentrations, the segment of experimental curve that is close to a given asymptote that is mostly governed by the constant that appears in the equation of the limiting behavior.

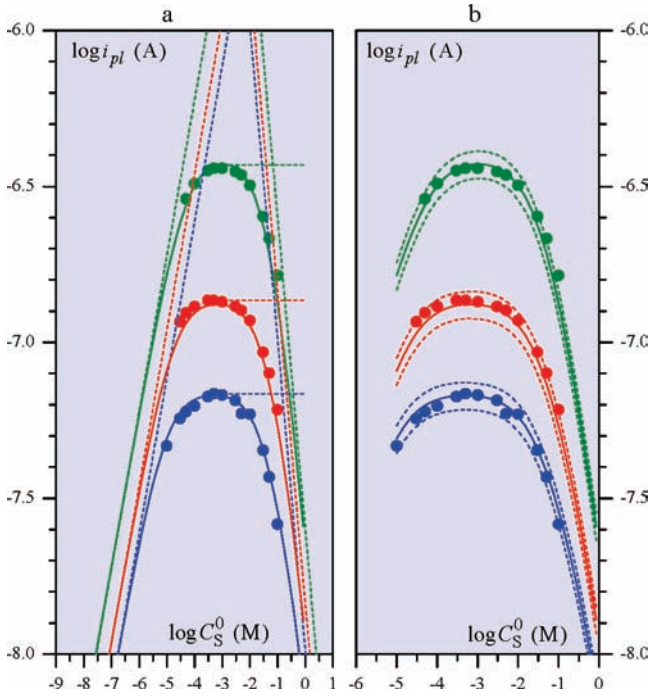

Figure 5. Variation of the plateau currents with substrate concentration at low mediator concentrations (blue: 0.5, red: 1, and green: 3 μM) in the presence of 94 nM of PQQ-GDH (wild type). Full lines: best fit of the experimental data by application of eq 1 with the constant values listed in Table 1. (a) Dotted horizontal lines: asymptotic behavior for $C_S^0 \rightarrow \infty$ with no inhibition (eq 2); left-hand ascending dashed lines: asymptotic behavior for $C_S^0 \rightarrow 0$ (eq 3); right-hand ascending dashed lines: asymptotic behavior for $C_S^0 \rightarrow \infty$ with inhibition (eq 4). (b) Dotted lines: upper and lower fitting corresponding to a 95% confidence interval based on twice the average standard deviation (10%) derived from three measurements.

The horizontal asymptote obtained for $C_S^0 \rightarrow \infty$ with no inhibition (horizontal dotted lines in Figure 5a) is given by

$$\frac{i_{pl}}{FS} = C_P^0\sqrt{2k_1C_E^0D_P}\sqrt{\frac{2}{\sigma}\left[1 - \frac{\ln(1+\sigma)}{\sigma}\right]} \quad \text{with}$$

$$\sigma = \frac{k_1C_P^0}{k_3} \qquad (2)$$

The height of the horizontal and its variation with C_P^0 thus allows the determination of k_1 and k_3.

The left-hand ascending asymptotes in Figure 5a, obey eq 3

$$\log\left(\frac{i_{pl}}{FS}\right) \xrightarrow{C_S^0 \rightarrow 0} \log\left(2\sqrt{D_PC_E^0C_P^0\frac{k_3}{K_M}}\right) + \frac{1}{2}\log C_S^0 \qquad (3)$$

from which k_3/K_M can be determined. Even though these asymptotes are not actually reached within the accessible range of concentrations, fitting of the left-hand part of the log i_{pl} vs log C_S^0 plot will allow the determination of k_3/K_M.

The effect of substrate inhibition appears in the right-hand descending portion of the log i_{pl} vs log C_S^0 plot. The pertinent

dx.doi.org/10.1021/ja204637d |J. Am. Chem. Soc. 2011, 133, 12801–12809

Table 1. Rate and Equilibrium Constants

	wild type	N428C mutant
From the Analysis of Reaction Triangle 1 (Low Mediator Concentrations)		
k_1 (M^{-1} s^{-1})	$(1.05 \pm 0.20) \times 10^8$	$(1.00 \pm 0.20) \times 10^8$
k_3 (s^{-1})	1500 ± 300	1500 ± 300
K_M (M)	$(4.6 \pm 1.8) \times 10^{-4}$	$(3.8 \pm 1.5) \times 10^{-4}$
$K_i = K_i'$ (M^{-1})	40 ± 5	35 ± 5
From the Analysis of Reaction Triangle 3 (High Mediator Concentrations)		
k_1'' (M^{-1} s^{-1})	$(1.10 \pm 0.15) \times 10^8$	$(1.05 \pm 0.20) \times 10^8$
k_3'' (s^{-1})	5000 ± 1000	$10\,000 \pm 1000$
K_M'' (M)	$(6.3 \pm 2.5) \times 10^{-3}$	$(14 \pm 4) \times 10^{-3}$
K_i'' (M^{-1})	65 ± 5	30 ± 5

asymptotic behavior is then given by eq 4:

$$\log\left(\frac{i_{pl}}{FS}\right) \xrightarrow{C_S^0 \to \infty} \log\left(2\sqrt{\frac{D_P C_E^0 C_P^0 k_3}{K_i K_i''}}\right) - \log C_S^0 \qquad (4)$$

showing that once k_3 is known, the two inhibition constants, K_i and K_i'' cannot be determined separately. To overcome this problem, K_i'' was derived from the analysis of reaction triangle 3 (see below), and K_i obtained from the fitting of the descending right-hand portion of the log i_{pl} vs log C_S^0 plot.

Having thus checked that the various portions of the log i_{pl} vs log C_S^0 plot contain enough information to allow the determination of all four constants, the final fitting with eq 1 of the experimental data shown in Figure 5b was obtained with the constant values listed in Table 1. Based on the standard deviation observed with three measurements for the same value of C_S^0, the ensuing bracketing of the curve fitting shown in Figure 5b led to the precision estimates reported in Table 1.

High Mediator Concentrations. If, by reference to Scheme 2, the mediator concentration is large enough to fulfill the following conditions: $C_P^0 > k_3/k_1''$ and k_{-2}/k_1'' and, at the same time, $C_S^0 > k_3'/k_2''$ and k_{-2}'/k_2'', the global reaction scheme simplifies so as to be reduced to the reaction triangle 3, as shown in Scheme 4. It is worth noting in passing that in this limiting case, only the reactions describing the cooperative effect are involved.

The same approach as for the reaction triangle 1, now applied to the reacting triangle 3, led to the constants listed in the bottom part of Table 1 by use of eq 5:

$$\frac{i_{pl}}{FSC_P^0} = \sqrt{\frac{2k_1'' C_E^0 D_P}{1 + K_i'' C_S^0}}\sqrt{\frac{2}{\sigma}\left[1 - \frac{\ln(1+\sigma)}{\sigma}\right]} \qquad (5)$$

with

$$\sigma = k_1'' C_P^0\left(\frac{1}{k_3''} + \frac{K_M''}{k_3'' C_S^0}\right)$$

That cooperativity exerts a strong effect on the kinetics is emphasized in Figure 6b, where it can be seen that the experimental data points stand much above the theoretical curves obtained with the constants derived for triangle 1 (Scheme 3).

Analysis of the Full Reaction Scheme. Once the constants have been determined from the limiting behaviors observed at low and high mediator concentrations, their validity can be tested by simulating the plateau currents over the whole range of mediator and substrate concentrations.[33] The results displayed in Figure 2 show a satisfactory adherence between simulated curves and experimental data, thus validating the reliability of the set of constants obtained by means of the limiting behavior approach.

Scheme 4

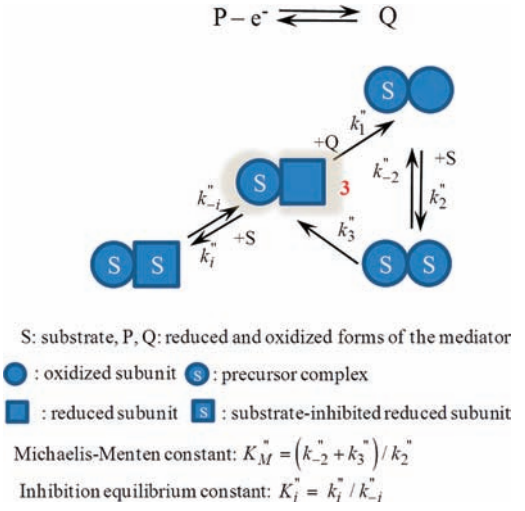

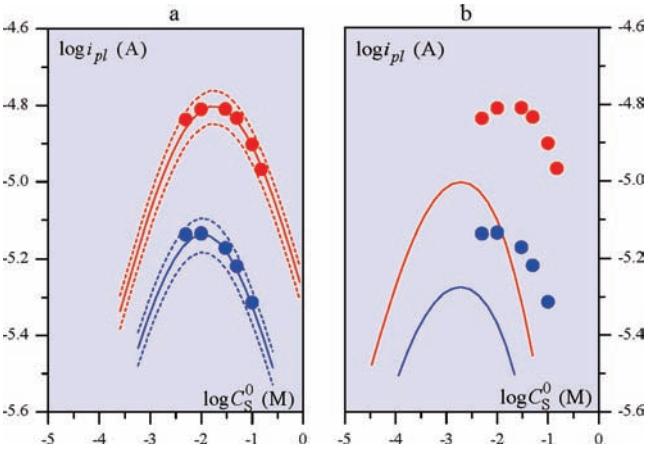

Figure 6. Variation of the plateau currents with substrate concentration at high mediator concentrations (blue: 100, red: 300 μM) in the presence of 94 nM of PQQ-GDH (wild type). (a) Full lines are the best fits of the experimental data by application of eq 5 with the constant values listed in Table 1. Dotted lines: upper and lower fitting corresponding to a 95% confidence interval based on twice the average standard deviation (10%) derived from three measurements. (b) Full lines: theoretical curves obtained by application of eq 1 with the constant values listed in Table 1 for triangle 1.

Catalysis by the N428C Mutant. As seen in Figures 3 and 4, there may be significant differences between the global catalytic reactivity of the wild and mutant (here the N428C mutant) types, depending on the mediator and the substrate concentrations; at low mediator concentration the global reactivity is slightly less for the mutant type than for the wild enzyme, whereas it is significantly higher for the mutant type than for the wild type at high mediator concentration, especially for high substrate

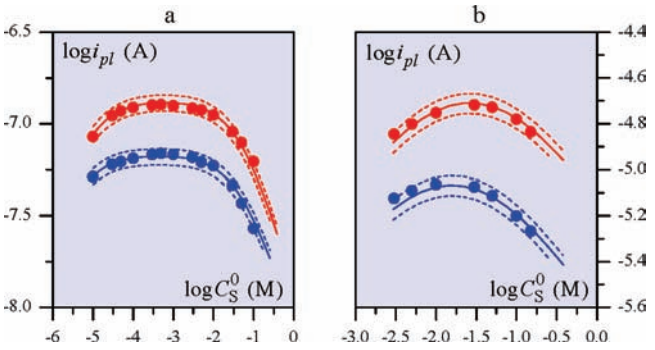

Figure 7. Variation of the plateau currents with substrate concentration at low (a: blue: 0.5, red: 1 μM) and high (b: blue: 100, red: 300 μM) mediator concentrations in the presence of 94 nM of PQQ-GDH (N428C mutant). Full lines: best fit of the experimental data by application of: (a) eq 1 and (b) eq 5 with the constant values listed in Table 1. Dotted lines: upper and lower fitting corresponding to a 95% confidence interval based on twice the average standard deviation (10%) derived from three measurements.

concentrations. These observations call for a full analysis of the mutant kinetics leading to the determination of all constants in the same way as was done for the wild type in order to spot the actual differences between the two types.

Figure 7 summarizes the application of the same fitting strategy as already used for the wild-type enzyme, leading to the constants of N428 mutant listed in Table 1.

CONCLUDING REMARKS

The kinetics of the catalytic oxidation of glucose by PQQ-GDH is complicated by substrate inhibition and cooperativity effects that add up to the Michaelis−Menten loops relative to substrate and mediator, as depicted in Scheme 2. The resulting kinetics is so much involved that it discourages the establishment of closed-form kinetic expressions or even formal expressions that would allow the grouping of the characteristics constants. Under these conditions, the determination of a reliably unique set of constants characterizing each elementary step involved in the Michaelis−Menten loops, substrate inhibition, and cooperativity requires a particularly watchful analysis. Based on simplifications suggested by extended knowledge previously acquired by standard spectroscopic kinetics, the electrochemical approach has allowed a detailed characterization that goes beyond what could be gathered by means of standard spectroscopic kinetics, particularly with regard to the reactions with the mediator and substrate inhibition.

The reason for such an achievement is the possibility to perform a large number of experiments using a single batch of enzyme solution unlike conventional kinetic methods, where a new batch has to be used for each mediator or substrate concentration. In addition, the sensitivity of the electrochemical technique allows the investigation of low substrate and mediator concentrations. Overall, data can be gathered over an extended range of substrate and mediator concentrations allowing the kinetic analysis of each step of the reaction, as exemplified in the present study. As concerns both the native and mutant enzymes, we note that substrate inhibition is quite substantial, leading to nonmonotonic glucose calibration curves. The catalytic current indeed starts to decrease for glucose concentrations above 0.1−1 mM in most cases. Cooperativity is also quite significant. The substrate turnover is 3−9 times larger when the neighboring subunit is filled with a glucose molecule, whereas the Michaelis−Menten constant is 6−30-fold higher.

Another practical illustration of the potentiality of the electrochemical approach is provided by the comparison of the constants characterizing the native and mutant enzymes. At low mediator concentrations, in the absence of cooperativity effects, the catalytic current responses are practically the same and so are the constants characterizing each individual step. Substantial differences appear at high mediator concentrations, where cooperativity takes place. Then, the catalytic current response of the mutant enzyme is significantly larger than for the native enzyme. The detailed electrochemical analysis identifies the reason for this improvement as deriving from a decrease of substrate inhibition by a factor 2 and a doubling of the overall turnover, leading to more than a doubling of the Michaelis−Menten constant. This is a starting example that may open a route to structure−reactivity relationships in PQQ-GDH and therefore to mutagenesis strategies aiming at improving the performances in terms of catalytic responses and/or substrate selectivity.

EXPERIMENTAL SECTION

Reagents. Pyrroloquinoline quinone (PQQ), D(+)-glucose, and bovine serum albumin (BSA) were purchased from Sigma (France) and used without further purification. Ferrocene methanol was also obtained from Sigma and recrystallized twice from toluene and cyclohexane. PQQ-dependent apo-glucose dehydrogenase (PQQ-dependent apo-GDH) from a recombinant *Escherichia coli* (E.C. 1.1.99.17) was purchased in lyophilized state from Genzyme (U.K.). PQQ-dependent apo-GDH mutated in position 428 by means of substitution of an asparagine amino acid by a cysteine residue (N428C) was constructed and purified as previously described.[21b] Salts for buffer solutions (Trizma, $Na_2HPO_4 \cdot 2\ H_2O$, $NaH_2PO_4 \cdot 2\ H_2O$, and $CaCl_2$) were obtained from Sigma. All other reagents were of analytical grade and used as received. Double-deionized water (18.2 MΩ cm, TKA Micro-Pure UV) was employed to prepare all aqueous solutions.

Three different buffers were used: TB (0.1 M of Tris−HCl, pH of 7.5), PB (0.1 M of phosphate buffer, pH of 7), enzyme reconstitution buffer (0.1 M of Tris−HCl, pH of 7.5, 3 mM of $CaCl_2$). In order to minimize adsorption of the enzyme on the electrochemical cell walls, 1 g/L of BSA was added to the corresponding solution that considerably increased the reproducibility of the results.

Instrumentation. Cyclic voltammetry and chronoamperometry measurements were performed with an AUTOLAB PGSTAT 12 potentiostat/galvanostat controlled by computer, and the data were acquired using GPES 4.9007 software (EcoChemie B.V. Utrecht, The Netherlands). The conventional three-electrode system was employed in all electrochemical studies. A saturated calomel electrode (SCE) and a platinum wire were used as reference and counter electrodes, respectively. Working electrodes were 4 mm diameter screen-printed carbon electrodes prepared using a commercial carbon ink (Electrodag PF-470 A), as previously described.[6c] The working area was rinsed with double-deionized water and subsequently modified with BSA by immersion for 15 min in PB buffer containing 0.1% BSA to avoid enzyme adsorption. All the electrochemical experiments were carried out at 20 ± 1 °C in a water-jacketed cell connected to a circulation thermostat (LAUDA M3). UV−vis absorption spectra were measured with a spectrophotometer Specord S600 (Analytic Jena).

Procedures. Glucose solutions were allowed to mutarotate to the anomeric equilibrium for one day before use in kinetic experiments. All kinetic data are expressed in terms of analytical glucose concentration although GDH is known to be specific for β-D-glucose.

The protocol for holo-GDH (native and mutant types) reconstitution from the corresponding apoform was adapted from reference.[13] Apo-GDH was rehydrated in 0.1 M of Tris−HCl pH of 7.5 buffer containing 3 mM of $CaCl_2$ and incubated with a 20-fold excess of PQQ with respect to subunit concentration for 2 h in the refrigerator (concentrations of both reagents were spectrophotometrically determined using the following specific absorption coefficients: 19 000 M^{-1} cm^{-1} at 250 nm for PQQ, and 1.28 L g^{-1} cm^{-1} for apo-GDH). PQQ excess was removed from the holoenzyme by centrifugation (11 000 × g, 30 min) using a Nanosep membrane with a molecular weight cut off of 10 kDa (Pall Corporation), equilibrated with TB pH of 7.5. Afterward, the enzyme was rinsed twice with TB pH of 7.5, once with PB pH of 7 and finally redispersed in PB pH of 7. UV−vis spectrum of the resulting solution showed a peak around 352 nm, which characterizes the incorporation of PQQ within the protein shell. Subsequent addition of 1 mM of glucose led to a shift of the maximum down to 338 nm, corresponding to the absorbance of the reduced form of bound PQQ (Figure 1S, Supporting Information). The absorbance ratio at 338 and 280 nm (A_{338}/A_{280}) of reduced holo-GDH was taken as an indicator of the relative amount of active enzyme. A value of 0.48 was found for both native and mutant holoforms, which is in agreement with that reported in reference 13 as well as with the electrochemical apoenzyme titration with PQQ in the presence of Ca^{2+} (Figure 2S, Supporting Information). Enzyme concentration was electrochemically titrated as well as determined using the extinction coefficient of 1.74 L g^{-1} cm^{-1} at 280 nm for reduced holo-GDH (Figure 2S, Supporting Information) and subsequently stored at −20 °C. Enzyme activities were measured as reported earlier (ref 21b).

■ ASSOCIATED CONTENT

Supporting Information. Establishment of eq 1, detailed description of the experimental procedures, and additional figures. This material is available free of charge via the Internet at http://pubs.acs.org.

■ AUTHOR INFORMATION

Corresponding Author
limoges@univ-paris-diderot.fr, saveant@univ-paris-diderot.fr

■ ACKNOWLEDGMENT

R.M.-C. thanks Fundación Ramón Areces for a postdoctoral grant. N.M. thanks the funding from a European Young Investigator Award (EURYI) and la Région Aquitaine

■ REFERENCES

(1) (a) Armstrong, F. A.; Wilson, G. S. *Electrochim. Acta* **2000**, *45*, 2623. (b) Wilson, G. S.; Hu, Y. *Chem. Rev.* **2000**, *100*, 2693. (c) Campbell, C. N.; Heller, A.; Caruana, D. J.; Schmidtke, D. W. In *Electroanalytical Methods for Biological Materials*; Brajter-Toth, A., Chambers, J. Q., Eds.; Marcel Dekker, Inc.: New York, 2002. (d) Alaejos, M. S.; Garcia Montelongo, F. J. *Chem. Rev.* **2004**, *104*, 3239. (e) Murphy, L. *Curr. Opin. Chem. Biol.* **2006**, *10*, 177. (f) Heller, A.; Feldman, B. *Chem. Rev.* **2008**, *108*, 2482.

(2) (a) Skladal, P. *Electroanalysis* **1997**, *9*, 737. (b) Warsinke, A.; Benkert, A.; Scheller, F. W. *Fresenius' J. Anal. Chem.* **2000**, *366*, 622. (c) Ghindilis, A. L.; Smith, M. W.; Schwarzkopf, K. R.; Roth, K. M.; Peyvan, K.; Munro, S. B.; Lodes, M. J.; Stöver, A. G.; Bernards, K.; Dill, K.; McShea, A. *Biosens. Bioeletron.* **2007**, *22*, 1853. (d) Sassolas, A.; Leca-Bouvier, B. D.; Blum, L. J. *Chem. Rev.* **2007**, *108*, 109.

(3) (a) Limoges, B.; Marchal, D.; Mavré, F.; Savéant, J.-M.; Schöllhorn, B. *J. Am. Chem. Soc.* **2008**, *130*, 7259. (b) Limoges, B.; Marchal, D.; Mavré, F.; Savéant, J.-M. *J. Am. Chem. Soc.* **2008**, *130*, 7276.

(4) (a) Calabrese Barton, S.; Gallaway, J.; Atanassov, P. *Chem. Rev.* **2004**, *104*, 4867. (b) Bullen, R. A.; Arnot, T. C.; Lakeman, J. B.; Walsh, F. C. *Biosens. Bioelectron.* **2006**, *21*, 2015. (c) Moehlenbrock, M. J.; Minteer, S. D. *Chem. Soc. Rev.* **2008**, *37*, 1188. (d) Cracknell, J. A.; Vincent, K. A.; Armstrong, F. A. *Chem. Rev.* **2008**, *108*, 2349. (e) Brito, P.; Turner, A. P. F. *Electroanalysis* **2010**, *22*, 732.

(5) (a) Bourdillon, C.; Demaille, C.; Moiroux, J.; Savéant, J.-M. *Acc. Chem. Res.* **1996**, *29*, 529. (b) Limoges, B.; Moiroux, J.; Savéant, J.-M. *J. Electroanal. Chem.* **2002**, *521*, 1. (c) Limoges, B.; Savéant, J.-M. *J. Electroanal. Chem.* **2003**, *549*, 61.(d) Savéant, J.-M. *Elements of Molecular and Biomolecular Electrochemistry: An Electrochemical Approach to Electron Transfer Chemistry*; John Wiley & Sons: Hoboken, NJ, 2006; Chap. 5.

(6) (a) Matsumoto, R.; Kano, K.; Ikeda, T. *J. Electroanal. Chem.* **2002**, *535*, 37. (b) Casero, E.; De Quesada, A.; Martinez, G.; Jin, J.; Quintana, M. C.; Pariente, F.; Abruña, H. D.; Vazquez, L.; Lorenzo, E. *Anal. Chem.* **2006**, *78*, 530. (c) Limoges, B.; Marchal, D.; Mavré, F.; Savéant, J.-M. *J. Am. Chem. Soc.* **2006**, *128*, 2084. (d) Fourmond, V.; Lagoutte, B.; Setif, P.; Leibl, W.; Demaille, C. *J. Am. Chem. Soc.* **2007**, *129*, 9201.

(7) (a) Limoges, B.; Yazidi, D.; Savéant, J.-M. *J. Am. Chem. Soc.* **2003**, *125*, 9122. (b) Calvente, J. J.; Narváez, A.; Domínguez, E.; Andreu, R. *J. Phys. Chem. B* **2003**, *107*, 6629.

(8) Cleton-Jansen, A.; Goosen, N.; Vink, K.; van de Putte, P. *Mol. Gen. Genet.* **1989**, *217*, 430.

(9) Oubrie, A.; Rozeboom, H.; Kalk, K. H.; Duine, J. A.; Dijkstra, B. W. *J. Mol. Biol.* **1999**, *289*, 319.

(10) Sato, A.; Takagi, K.; Kano, K.; Kato, N.; Duine, J. A.; Ikeda, T. *Biochem. J.* **2001**, *357*, 893.

(11) Olsthoorn, A. J. J.; Otsuki, T.; Duine, J. A. *Eur. J. Biochem.* **1997**, *247*, 659.

(12) (a) Hauge, J. G. *J. Biol. Chem.* **1964**, *239*, 3630. (b) Dokter, P.; Frank, J. J.; Duine, J. A. *Biochem. J.* **1986**, *239*, 163. (c) Geiger, O.; Görisch, H. *Biochemistry* **1986**, *25*, 6043.

(13) Olsthoorn, A. J. J.; Duine, J. A. *Arch. Biochem. Biophys.* **1996**, *336*, 42.

(14) Olsthoorn, A. J. J.; Otsuki, T.; Duine, J. A. *Eur. J. Biochem.* **1998**, *255*, 255.

(15) (a) Weibel, M. K.; Bright, H. *J. Biol. Chem.* **1971**, *246*, 2734. (b) Bourdillon, C.; Demaille, C.; Moiroux, J.; Savéant, J.-M. *J. Am. Chem. Soc.* **1993**, *115*, 2.

(16) D'Costa, E. J.; Higgins, I. J.; Turner, A. P. F. *Biosensors* **1986**, *2*, 71.

(17) Okuda, J.; Wakai, J.; Yuhashi, N.; Sode, K. *Biosens. Bioelectron.* **2003**, *18*, 699.

(18) (a) Ye, L.; Haemmerle, M.; Olsthoorn, A. J. J.; Schuhmann, W.; Schmidt, H. L.; Duine, J. A.; Heller *Anal. Chem.* **1993**, *65*, 238. (b) Habermuller, K.; Ramanavicius, A.; Laurinavicius, V.; Schuhmann, W. *Electroanalysis* **2000**, *12*, 1383. (c) Tsujimura, S.; Katayama, A.; Kano, K. *Chem. Lett.* **2006**, *35*, 1244. (d) Lau, C.; Borgmann, S.; Maciejewska, M.; Ngounou, B.; Gründler, P.; Schuhmann, W. *Biosens. Bioelectron.* **2007**, *22*, 3014. (e) Nagel, B.; Warsinke, A.; Katterle, M. *Langmuir* **2007**, *23*, 6807.

(19) (a) Newman, J. D.; Turner, A. P. F. *Biosens. Bioelectron.* **2005**, *20*, 2435. (b) Yoo, E.-H.; Lee, S.-Y. *Sensors* **2010**, *10*, 4558.

(20) (a) Yamazaki, T.; Kojima, K.; Sode, K. *Anal. Chem.* **2000**, *72*, 4689. (b) Igarashi, S.; Hirokawa, T.; Sode, K. *Biomol. Engineering* **2004**, *21*, 81. (c) Igarashi, S.; Okuda, J.; Ikebukuro, K.; Sode, K. *Arch. Biochem. Biophys.* **2004**, *428*, 52. (d) Hamamatsu, N.; Suzumura, A.; Nomiya, Y.; Sato, M.; Aita, T.; Nakajima, M.; Husimi, Y.; Shibanaka, Y. *Appl. Microbiol. Biotechnol.* **2006**, *73*, 607.

(21) (a) Igarashi, S.; Ohtera, T.; Yoshida, H.; Witarto, A. B.; Sode, K. *Biochem. Biophys. Res. Commun.* **1999**, *264*, 820. (b) Durand, F.; Stines-Chaumeil, C.; Flexer, V.; André, I.; Mano, N. *Biochem. Biophys. Res. Commun.* **2010**, *402*, 750.

(22) (a) Sode, K.; Ohtera, T.; Shirahane, M.; Witarto, A. B.; Igarashi, S.; Yoshida, H. *Enzyme Microb. Technol.* **2000**, *26*, 491. (b) Igarashi, S.; Sode, K. *Mol. Biotechnol.* **2003**, *24*, 97.

(23) (a) Kulys, J.; Tetianec, L. *Sens. Actuators, B* **2006**, *113*, 755. (b) Weber, C.; Gauda, E.; Mizaikoff, B.; Kranz, C. *Anal. Bioanal. Chem.* **2009**, *395*, 1729.

(24) Ikebukuro, K.; Kohiki, Y.; Sode, K. *Biosens. Bioelectron.* **2002**, *17*, 1075.

(25) Ikebukuro, K.; Kiyohara; Sode, K. *Biosens. Bioelectron.* **2005**, *20*, 2168.

(26) (a) Shen, D.; Meyerhoff, M. E. *Anal. Chem.* **2009**, *81*, 1564. (b) Zimmerman, L. B.; Lee, K.-D.; Meyerhoff, M. E. *Anal. Biochem.* **2010**, *401*, 182.

(27) (a) Jin, W.; Bier, F.; Wollenberger, U.; Scheller, F. *Biosens. Bioelectron.* **1995**, *10*, 823. (b) Bauer, C. G.; Eremenko, A. V.; Ehrentreich-Förster, E.; Bier, F. F.; Makower, A.; Halsall, H. B.; Heineman, W. R.; Scheller, F. W. *Anal. Chem.* **1996**, *68*, 2453. (c) Szeponik, J.; Möller, B.; Pfeiffer, D.; Lisdat, F.; Wollenberger, U.; Makower, A.; Scheller, F. W. *Biosens. Bioelectron.* **1997**, *12*, 947. (d) Lisdat, F.; Wollenberger, U.; Paeschke, M.; Scheller, F. W. *Anal. Chim. Acta* **1998**, *368*, 233.

(28) (a) Tsujimura, S.; Kano, K.; Ikeda, T. *Electrochemistry* **2002**, *70*, 940. (b) Yuhashi, N.; Tomiyama, M.; Okuda, J.; Igarashi, S.; Ikebukuro, K.; Sode, K. *Biosens. Bioelectron.* **2005**, *20*, 2145. (c) Hao, Yu, E.; Scott, K. *Energies* **2010**, *3*, 23. (d) Tanne, C.; Göbel, G.; Lisdat, F. *Biosens. Bioelectron.* **2010**, *26*, 530.

(29) (a) Matsushita, K.; Shinagawa, E.; Adachi, O.; Ameyama, M. *FEMS Microbiol. Lett.* **1988**, *55*, 53. (b) Olsthoorn, A. J. J.; Duine, J. A. *Biochemistry* **1998**, *37*, 13854.

(30) Savéant, J.-M. *Elements of Molecular and Biomolecular Electrochemistry: An Electrochemical Approach to Electron Transfer Chemistry*; John Wiley & Sons: Hoboken, NJ, 2006. Chap. 2.

(31) (a) Duine, J. A. *Eur. J. Biochem.* **1991**, *200*, 271–284. (b) Duine, J. A. *J. Biosci. Bioeng.* **1999**, *88*, 231. (c) Dokter, P.; Frank, J.; Duine, J. A. *Biochem. J.* **1986**, *239*, 163–167.

(32) As determined from the cyclic voltammetric response of ferrocene methanol in the conditions of the present study, which are the same as in ref 10.

(33) Using the Digielch software: Rudolph, M. *J. Electroanal. Chem.* **2003**, *543*, 23.